Oscillatory shear response of dilute ferrofluids: Predictions from rotational Brownian dynamics simulations and ferrohydrodynamics modeling

D. Soto-Aquino, D. Rosso, and C. Rinaldi*

Department of Chemical Engineering, University of Puerto Rico, Mayagüez, P. O. Box 9000, Mayagüez Puerto Rico 00681

(Received 30 June 2011; published 14 November 2011)

Ferrofluids are colloidal suspensions of magnetic nanoparticles that exhibit normal liquid behavior in the absence of magnetic fields but respond to imposed magnetic fields by changing their viscosity without loss of fluidity. The response of ferrofluids to constant shear and magnetic fields has received a lot of attention, but the response of ferrofluids to oscillatory shear remains largely unexplored. In the present work we used rotational Brownian dynamics to study the dynamic properties of ferrofluids with thermally blocked nanoparticles under oscillatory shear and constant magnetic fields. Comparisons between simulations and modeling using the ferrohydrodynamics equations were also made. Simulation results show that, for small rotational Péclet number, the in-phase and out-of-phase components of the complex viscosity depend on the magnitude of the magnetic field and frequency of the shear, following a Maxwell-like model with field-dependent viscosity and characteristic time equal to the field-dependent transverse magnetic relaxation time of the nanoparticles. Comparison between simulations and the numerical solution of the ferrohydrodynamic equations shows that the oscillatory rotational magnetoviscosity for an oscillating shear field obtained using the kinetic magnetization relaxation equation quantitatively agrees with simulations for a wide range of Péclet number and Langevin parameter but has quantitative deviations from the simulations at high values of the Langevin parameter. These predictions indicate an apparent elastic character to the rheology of these suspensions, even though we are considering the infinitely dilute limit in which there are negligible particle-particle interactions and, as such, chains do not form. Additionally, an asymptotic analytical solution of the ferrohydrodynamics equations, valid for $\mathrm{Pe} \ll 2$, was used to demonstrate that the Cox-Merz rule applies for dilute ferrofluids under conditions of small shear rates. At higher shear rates the Cox-Merz rule ceases to apply.

DOI: 10.1103/PhysRevE.84.056306 PACS number(s): 47.57.Qk, 47.65.Cb

I. INTRODUCTION

Ferrofluids are colloidal suspensions of nanosized magnetic particles in a simple carrier fluid which respond to an external magnetic field with changes in their rheological properties [1–4]. The magnetorheology of ferrofluids has been an active area of experimental [1–6] and theoretical [7–12] research for decades. The focus of most work has been the steady-state response of dilute and semidilute ferrofluids to imposed constant shear and magnetic fields [2,3,13–21]. There has also been some work on the response of ferrofluids to oscillating [3,14,22–26] and rotating [14,27–32] magnetic fields; however, here again a steady flow has been considered. Recently, the dynamics of the transient magnetoviscous effect has received attention [33,34], with emphasis on response of ferrofluids to step changes in the applied magnetic or shear fields.

Surprisingly, the response of ferrofluids to oscillating shear fields seems to have received little attention, even though oscillatory shear experiments are common rheological tools to study complex fluids [35–37]. In these measurements, both stress and strain vary cyclically with time, with sinusoidal variation being the most commonly used. The cycle time, or frequency of oscillation, defines the time scale of the test. Thus, by observing material response as a function of frequency, mechanical properties can be probed at different time scales. Klingenberg [38,39] used molecular dynamics to study the oscillatory shear response of electrorheological suspensions composed of dielectric spheres in a Newtonian fluid between parallel-plate electrodes. The response obtained was described by frequency-dependent moduli determined by a competition between hydrodynamic and electrostatic interactions that dominate chain formation, deformation, and breakage. A similar response was predicted for magnetorheological (MR) fluids, concentrated suspensions of micron-sized magnetizable particles, and expressed as a relation between magnetic and hydrodynamic forces using the so-called Mason number [40]. Kanai and Amari [41] studied flocculated suspensions of micron-sized ferric oxide particles in mineral oil. They found strain-thickening behavior one decade larger than in the nonmagnetic-based oil, which they attributed to particle-particle interactions. Li *et al.* [42] studied the dynamic behavior of MR fluids under oscillatory shear. Linear viscoelastic behavior was observed in these fluids only at very small strain amplitudes, and the response could be captured using a Pipkin diagram describing the rheological behavior as a function of strain amplitude and frequency. Claracq *et al.* [37] used micron-sized colloidal magnetic particles coated with latex to study the viscoelastic behavior of MR fluids subjected to small deformations. They related the magnetic force to the elastic modulus using a Mason number and compared their results with those obtained by Klingenberg [38,39] using simulations. They found that the application of a magnetic field causes aggregation of the particles into chains in the magnetic field direction and that these were destroyed when high shear rates perpendicular to the magnetic field were applied. de Gans *et al.* [43] investigated an MR fluid consisting of colloidal

*carlos.rinaldi@upr.edu

silica spheres suspended in an organic ferrofluid; a so-called inverse ferrofluid. They found that the storage modulus G' was an order of magnitude larger than the loss modulus G'' at all magnetic fields studied. In addition, a model considering a collection of noninteracting spherical particles was derived for the high-frequency limit of the storage modulus. Ramos *et al*. [36] also used a silica-based inverse ferrofluid to study the magnetorheology behavior under small-amplitude oscillatory shear in the presence of an external magnetic field. Their results were compared with those of de Gans *et al*. [43,44] and chain models and excellent agreement was obtained.

For many systems the steady-state viscosity is difficult to measure at high shear rate. Data obtained from oscillatory experiments are usually more reliable and the Cox-Merz rule has been used to predict the viscosity at a steady shear rate $\eta(\dot{\gamma})$ from oscillatory measurements. Although only partial justification for the Cox-Merz rule has been provided [45], the Cox-Merz rule has been found to hold for many polymer melts and concentrated and semidilute solutions [35]. Recently, Chae and collaborators [46] demonstrated that the Cox-Merz rule was inapplicable to concentrated dispersions of asymmetric magnetic particles. However, they studied a magnetic dispersion of particles with average length of 350 nm which tends to form aggregates and clusters which are difficult to destroy even at high shear rates. Thus, the applicability of the so-called Cox-Merz rule to ferrofluids remains an open question.

Asthe reviewed literature indicates, oscillatory shear experiments have resulted in important insight into the dynamics of magnetorheological fluids and flocculated suspensions for which the viscoelastic moduli seem to depend primarily on the dynamics and mechanics of chain formation, deformation, and breakage. Surprisingly, oscillatory shear experiments have received little application in the study of ferrofluids, even though chain formation, deformation, and breakage are also important processes that determine the magnetorheological properties of ferrofluids [47]. Recently, Pinho *et al*. [48] reported a series of oscillatory shear measurements with commercial ferrofluids in applied magnetic fields. They only reported viscous damping of the force on an oscillating plate in contact with ferrofluid subjected to a constant magnetic field. The viscous damping and associated viscosity increased with magnetic field and monotonically decreased with oscillation frequency, which was limited to 10–50 Hz. Under the conditions of this study the ferrofluid apparently did not display an elastic contribution in the response to the oscillatory shear. Furthermore, the authors did not provide detailed physical or magnetic characterization of the fluid, making interpretation of their results difficult, and did not attempt to model the observed behavior. Still their contribution is significant as it appears to be the first application of oscillatory techniques to the study of ferrofluids.

In this contribution we study the dynamic magnetoviscosity of a ferrofluid, composed of noninteracting spherical permanently magnetized particles subjected to a constant magnetic field and an oscillatory shear flow described by

$$\dot{\gamma} = \frac{dv_y}{dz} = \dot{\gamma}_0 \sin(\Omega t). \tag{1}$$

To do so we apply rotational Brownian dynamics simulations in the inertialess limit and compare these to predictions obtained from the ferrohydrodynamic equations using the kinetic magnetization equation of Martsenyuk, Raikher, and Shliomis [9]. In Sec. II we introduce the methodology for the rotational Brownian dynamics simulations; in Sec. III we discuss analytical and numerical approaches to the problem using the ferrohydrodynamics equations and the kinetic magnetization relaxation equation; in Sec. IV we present and discuss our results; in Sec. V we consider the applicability of the Cox-Merz rule for ferrofluids in the infinitely dilute limit; and in Sec. VI we provide our concluding remarks.

II. ROTATIONAL BROWNIAN DYNAMICS

Rotational Brownian dynamics simulations are based on the integration of the stochastic angular momentum equation to obtain the evolution in orientation of each particle assuming that inertia is negligible—a suitable assumption for the particle sizes in ferrofluids. Here we are concerned with infinitely dilute ferrofluids wherein there are no magnetic or hydrodynamic particle-particle interactions. There are three kinds of torque acting on the particle: $\mathbf{T}_h$ due to hydrodynamic drag, $\mathbf{T}_m$ due to the effect of magnetic fields, and $\mathbf{T}_B$ due to Brownian motion. The torque due to hydrodynamic drag is given by

$$\mathbf{T}'_h = -\eta_0\left[K_r\left(\omega' - \tfrac{1}{2}\nabla \times \mathbf{v}'\right)\right], \tag{2}$$

where η_0 is the viscosity of the carrier fluid, $K_r = 8\pi r^3$ is the hydrodynamic rotational resistance coefficient, and ω' and $\frac{1}{2}\nabla \times \boldsymbol{v}'$ are the angular velocity of the particle and the fluid, respectively. The unperturbed flow velocity $\mathbf{v}$, and the vorticity of the fluid $\boldsymbol{\omega}_f$ are given by

$$\begin{aligned} \mathbf{v} &= \dot{\gamma}(t)\, z\mathbf{i}_y = \dot{\gamma}_0 \sin(\Omega t)\, z\mathbf{i}_y, \\ \omega_f &= -\tfrac{1}{2}\dot{\gamma}(t)\,\mathbf{i}_x = -\tfrac{1}{2}\dot{\gamma}_0 \sin(\Omega t)\,\mathbf{i}_x. \end{aligned} \tag{3}$$

The magnetic torque is given by

$$\mathbf{T}_m g = \mu_0(\mathbf{m}' \times \mathbf{H}'), \tag{4}$$

where μ_0 is the permeability of free space, $\mathbf{m} = m\boldsymbol{\mu}'$ is the magnetic dipole moment of the particle, and $\mathbf{H}' = \mathbf{A}\cdot\mathbf{H}$ is the applied magnetic field, transformed to the body-fixed axis using the transformation matrix **A,** written in our case in terms of the Euler parameters [13,49]. In our simulations the magnetic dipole moment of the particle $bm\mu'$ is directed along the z' axis, the simple shear flow is along the y axis, and the magnetic field $\mathbf{H}$ is along the z axis. Primes indicate a vector with respect to particle-locked coordinates.

In order to reduce the number of variables in the angular momentum equation, time was nondimensionalized with respect to the rotational diffusion coefficient $D_r = k_B T(\eta_0 K_r)^{-1}$, and the vector variables were nondimensionalized with respect to their magnitudes [15]. Setting $d\tilde{\boldsymbol{\Phi}}' = \tilde{\boldsymbol{\omega}}' d\tilde{t}$, where $d\tilde{\boldsymbol{\Phi}}'$ is the infinitesimal rotation vector, integrating from time $\tilde{t}$ to $\tilde{t} + \Delta\tilde{t}$ using a first-order forward Euler method and applying the fluctuation-dissipation theorem to the Brownian term [50], we obtain

$$\Delta\tilde{\boldsymbol{\Phi}}' = \alpha(\tilde{\mu}' \times \tilde{\mathbf{H}}')\Delta\tilde{t} - \mathbf{Pe}\,\sin(\tilde{\Omega}\Delta\tilde{t})\tilde{\boldsymbol{\omega}}'_f\Delta\tilde{t} + \tilde{\mathbf{w}}'. \tag{5}$$

In Eq. (5), $\alpha = mH/(k_B T)$ is the Langevin parameter and $\mathrm{Pe} = \dot{\gamma}_0/D_r$ is the rotational Péclet number. The vector $\tilde{\mathbf{w}}'$ is

a random vector which follows a Gaussian distribution with mean and covariance given by

$$\langle \tilde{\mathbf{w}}_i' \rangle = 0, \quad \langle \tilde{\mathbf{w}}_i' \tilde{\mathbf{w}}_i' \rangle = 2\mathbf{I}\Delta\tilde{t}. \tag{6}$$

The algorithm proceeds from a starting configuration by calculating the change in orientation at each time step. Orientation is represented through the quaternion parameters e_0, e_1, e_2, and e_3. Changes in the quaternion parameters are related to Eq. (5) through [15]

$$\begin{bmatrix} \Delta e_0 \\ \Delta e_1 \\ \Delta e_2 \\ \Delta e_3 \end{bmatrix} = \frac{1}{2} \begin{bmatrix} e_0 & -e_1 & -e_2 & -e_3 \\ e_1 & e_0 & -e_3 & e_2 \\ e_2 & e_3 & e_0 & -e_1 \\ e_3 & -e_2 & e_1 & e_0 \end{bmatrix} \begin{bmatrix} 0 \\ \Delta\tilde{\Phi}_x' \\ \Delta\tilde{\Phi}_y' \\ \Delta\tilde{\Phi}_z' \end{bmatrix}. \tag{7}$$

After each time step, the quaternion parameters of each particle are normalized. All runs were performed starting from a random configuration, using 10^5 noninteracting particles. The system is stabilized at constant magnetic field and zero shear until it reaches equilibrium, typically after $\tilde{t}$ =10. At this point the oscillatory shear is turned on. A time step of $\tilde{t} = 0.0005$ was used in order to observe the fastest processes in the system in a frequency range of $0.01 < \tilde{\Omega} < 100.0$. Langevin parameters of $\alpha = 0.1$, 1.0, and 10.0, and dimensionless shear rates of Pe = 1.0, 5.0, and 10.0 were used.

The apparent viscosity of the suspension due to the antisymmetric part of the viscous stress tensor is given by $\eta_{zy}^m = \tau_{zy}^a/\dot{\gamma}$, which is referred to as the magnetoviscosity of the suspension. The antisymmetric part of the stress tensor can be obtained from $\boldsymbol{\tau}^a = -\frac{n}{2}\langle \boldsymbol{\varepsilon} \cdot \mathbf{T}_m \rangle$, where n is the number of particles and ε is the alternating unit tensor [15]. For a dilute suspension, the intrinsic magnetoviscosity $[\eta_{zy}^m]$ is defined as

$$[\eta_{zy}^m] = \lim_{\phi \to 0} \frac{\eta_{zy}^m}{\phi \eta_0}. \tag{8}$$

Using the transformation matrix, the magnetoviscosity equation is expressed in terms of the quaternion parameters. The resulting equation is [15]

$$[\eta_{zy}^m] = -3\frac{\alpha}{\mathrm{Pe}} \langle 2(e_2 e_3 - e_0 e_1)\tilde{H}_z \rangle_{zy}. \tag{9}$$

Because an oscillating shear is applied, one would expect a time-periodic magnetoviscosity. When α and Pe are small (i.e., not far from equilibrium) one would expect the response for a sinusoidal shear such as Eq. (1) to be equally sinusoidal but with a phase lag. On the other hand, for large values of α and Pe, one would expect deviations from sinusoidal response but still time-periodic behavior. To parameterize the dynamic magnetoviscosity we introduce the nth-order in-phase η_n' and out-of-phase η_n' viscosities using a Fourier series representation of the time-dependent pseudo-steady intrinsic magnetoviscosity

$$[\eta_{zy}^m] = \sum_{n=1}^{\infty} \eta_{m,n}' \sin(n\Omega t) + \sum_{n=1}^{\infty} \eta_{m,n}'' \cos(n\Omega t). \tag{10}$$

The nth-order in-phase and out-of-phase dynamic viscosities can be obtained from

$$\begin{aligned} \eta_{m,n}' &= \frac{1}{\pi} \int_{-\pi}^{\pi} \tilde{\eta}(t) \sin(n\Omega t)\, d(\Omega t), \\ \eta_{m,n}'' &= \frac{1}{\pi} \int_{-\pi}^{\pi} \tilde{\eta}(t) \cos(n\Omega t)\, d(\Omega t). \end{aligned} \tag{11}$$

For low values of α and Pe, we expect purely sinusoidal behavior and, as such, $\eta_n' = 0$, $\eta_n'' = 0$ for $n > 1.0$. However, for large α and Pe, we expect deviations from sinusoidal behavior, captured by $\eta_{m,n}' \neq 0$ and $\eta_{m,n}'' \neq 0$ with $n > 1.0$. Although Eq. (11) defines $\eta_{m,n}'$ and $\eta_{m,n}''$ for any order of n, we will focus only on $n = 1$ when analyzing the simulation results, as these are the quantities typically measured in oscillatory shear experiments. In that case we write η_m' and η_m'' for the components of the dynamic magnetoviscosity.

III. CONTINUUM MODELING

For ferrofluids consisting of particles with rigidly locked magnetic dipoles suspended in an incompressible fluid in the infinitely dilute limit, the commonly accepted governing ferrohydrodynamics equations are [51]

$$\nabla \cdot \mathbf{v} = 0, \tag{12}$$

$$\rho \frac{D\mathbf{v}}{Dt} = \mu_0 \mathbf{M} \cdot \nabla \mathbf{H} - \nabla p + 2\zeta \nabla \times \boldsymbol{\omega} + \eta_e \nabla^2 \mathbf{v}, \tag{13}$$

$$0 = \mu_0 \mathbf{M} \times \mathbf{H} + 2\zeta \nabla \times \mathbf{v} - 4\zeta\omega. \tag{14}$$

Here, $\mathbf{v}$ is the mass-average velocity, ρ is the fluid density, $\mathbf{M}$ is the suspension magnetization, $\mathbf{H}$ is the magnetic field, p is the fluid pressure, ζ is the so-called vortex viscosity, $\boldsymbol{\omega}$ is the ferrofluid spin velocity, and $\eta_e = \eta + \zeta$ is an effective viscosity with η being the shear viscosity of the ferrofluid. Note that, in Eq. (13), we have left out the term corresponding to the couple stress and the controversial spin viscosity [27–29,52–54]. This is justified because we are considering here the limit of infinite dilution for which there are no particle-particle magnetic or hydrodynamic interactions and hence no mechanism for transport of internal angular momentum. We have also left out the term corresponding to the moment-of-inertia density of the nanoparticles, which is a good assumption owing to the small particle size typical of ferrofluids.

Martsenyuk, Raikher, and Shliomis [9] proposed a magnetization relaxation equation, denoted here as the MRS equation, derived microscopically from the Fokker-Planck equation. This equation has been found to well describe the magnetic field and shear-rate dependence of the magnetoviscosity of dilute ferrofluids [13]. The equation is derived using an effective-field method which results in closure of the first moment of magnetization, yielding

$$\frac{d\mathbf{M}}{dt} = \boldsymbol{\Omega} \times \mathbf{M} - \frac{\mathbf{H}[\mathbf{H} \cdot (\mathbf{M} - \mathbf{M}_{\mathrm{eq}})]}{\tau_{\parallel} H^2} - \frac{\mathbf{H} \times (\mathbf{M} \times \mathbf{H})}{\tau_{\perp} H^2}. \tag{15}$$

Here, $\mathbf{M}$ stands for the ferrofluid magnetization due to the magnetic field $\mathbf{H}$ and the flow vorticity $\boldsymbol{\Omega} = \frac{1}{2}\nabla \times \mathbf{v}$.

At equilibrium in a stationary field, $\mathbf{M}_{\rm eq}$ is described by the Langevin function $L(\alpha)$:

$$\begin{aligned}\mathbf{M}_{\rm eq} &= nmL(\alpha)\frac{\mathbf{H}}{H} = M_s(\coth\alpha - \alpha^{-1})\mathbf{i}_z,\\ \alpha &= \frac{mH}{k_BT}, \quad L(\alpha) = \coth\alpha - \alpha^{-1},\end{aligned} \tag{16}$$

where m is the magnetic dipole moment of an individual particle, n is the number density of the particles, and α is the Langevin parameter.

The parallel $\tau_\parallel$ and transverse $\tau_\perp$ relaxation times of Eq. (15) are given by

$$\tau_\parallel = \frac{d\ln L(\alpha)}{d\ln\alpha}, \quad \tau_\perp = \frac{2L(\alpha)}{\alpha - L(\alpha)}\tau, \tag{17}$$

with

$$\tau = \frac{3\eta V}{k_BT} \tag{18}$$

being the characteristic Brownian relaxation time of rotational particle diffusion.

The system under consideration will be assumed to be of infinite extent; that is, we will ignore the effect of boundaries and transients associated with momentum diffusion. As such, all spatial derivatives are zero, except for those of the translational velocity that satisfies the condition of simple shear flow in Eq. (3). In the following, we will limit our attention to the case of a unidirectional applied magnetic field, $\mathbf{H} = H_0\mathbf{i}_z$and the oscillating simple shear flow of Eq. (3). Maxwell's equations in the magnetoquasistatic limit are obeyed; however, these are trivially satisfied by the imposed magnetic field and flow. In this case the simple shear flow will result in a magnetization which lies in the yz plane, hence we have $\mathbf{M} = M_y(t)\mathbf{i}_y + M_z(t)\mathbf{i}_z$. Therefore, in component form, Eq. (15) becomes

$$\begin{aligned}\frac{\partial M_y}{\partial t} &= \frac{1}{2}\dot\gamma(t)M_z(t) - \frac{M_y}{\tau_\perp},\\ \frac{\partial M_z}{\partial t} &= -\frac{1}{2}\dot\gamma(t)M_y(t) - \frac{[M_z(t) - M_sL(\alpha)]}{\tau_\parallel}.\end{aligned} \tag{19}$$

In order to facilitate the analysis and comparisons with the results of Brownian dynamics simulations we introduce the dimensionless quantities

$$\begin{aligned}\tilde t &= \frac{t}{2\tau}, \quad \tilde\tau_\perp = \frac{\tau_\perp}{2\tau}, \quad \tilde\tau_\parallel = \frac{\tau_\parallel}{2\tau},\\ {\rm Pe} &= 2\dot\gamma_0\tau, \quad \varepsilon = \frac{\rm Pe}{2},\\ f(\tilde t) &= \frac{M_y}{M_sL(\alpha)}, \quad g(\tilde t) = \frac{M_z}{M_sL(\alpha)},\\ {\rm Mn} &= \frac{\zeta\dot\gamma}{\mu_0M_sL(\alpha)H_0},\end{aligned} \tag{20}$$

where Mn is a form of the Mason number (i.e., the ratio between the viscous and magnetic stresses [55,56]). Substituting (20) in (19) we obtain

$$\begin{aligned}\frac{\partial f}{\partial t} &= \varepsilon\sin(\tilde\Omega\tilde t)g(\tilde t) - \frac{1}{\tilde\tau_\perp}f(\tilde t),\\ \frac{\partial g}{\partial t} &= -\varepsilon\sin(\tilde\Omega\tilde t)f(\tilde t) - \frac{1}{\tilde\tau_\parallel}[g(\tilde t) - 1],\end{aligned} \tag{21}$$

with the initial conditions $f(t=0) = 0$ and $g(t=0) = 1$. In general, Eq. (21) has to be solved numerically. However, first we obtain an asymptotic analytical solution in order to gain physical insight.

A. Regular perturbation solution

To solve Eq. (21) analytically we apply a regular perturbation expansion in the small parameter $\varepsilon = \frac{\rm pe}{2} < 1$, with the form

$$f(t) = \sum_{n=0}^{\infty}\varepsilon^n f_n(t), \quad g(t) = \sum_{n=0}^{\infty}\varepsilon^n g_n(t). \tag{22}$$

Equation (22) is introduced into Eq. (21) and each term is expanded to obtain an equation in power series of ε. The nth-order problem corresponds to the terms multiplied by ε^n. Each of these problems can be solved in turn and the solutions added to obtain a power-series approximation to the actual solution.

The zeroth-order problem is given by

$$\begin{aligned}\frac{\partial f_0}{\partial t} &= -\frac{1}{\tilde\tau_\perp}f_0(\tilde t), \quad f_0(0) = 0,\\ \frac{\partial g_0}{\partial t} &= -\frac{1}{\tilde\tau_\parallel}[g_0(\tilde t) - 1], \quad g_0(0) = 1,\end{aligned} \tag{23}$$

with the solution

$$f_0(\tilde t) = 0, \quad g_0(\tilde t) = 1, \tag{24}$$

corresponding to equilibrium. The transient approach to this pseudosteady equilibrium state could be obtained but is not relevant because we seek to understand the pseudosteady response at long times.

The first-order problem is given by

$$\begin{aligned}\frac{\partial f_1}{\partial\tilde t} &= \sin(\tilde\Omega\tilde t)g_o(\tilde t) - \frac{1}{\tilde\tau_\perp}f_1(\tilde t), \quad f_1(0) = 0,\\ \frac{\partial g_1}{\partial\tilde t} &= -\frac{1}{\tilde\tau_\parallel}g_1(\tilde t), \quad g_1(0) = 0.\end{aligned} \tag{25}$$

This system of equations is solved to obtain

$$f_1(\tilde t) = \tilde\tau_\perp\frac{\sin(\tilde\Omega\tilde t) - \tilde\Omega\tilde\tau_\perp\cos(\tilde\Omega\tilde t)}{(1+\tilde\tau_\perp^2\tilde\Omega^2)}, \quad g_1(\tilde t) = 0. \tag{26}$$

The second-order problem is given by

$$\frac{\partial f_2}{\partial\tilde t} = -\frac{1}{\tilde\tau_\perp}f_2(\tilde t), \quad \frac{\partial g_2}{\partial\tilde t} = -\sin(\tilde\Omega\tilde t)f_1(\tilde t) - \frac{1}{\tilde\tau_\parallel}g_2(\tilde t), \tag{27}$$

which results in

$$f_2(\tilde{t}) = 0, \quad g_2(\tilde{t}) = \frac{\tilde{\tau}_\parallel \tilde{\tau}_\perp [-1 - 4\tilde{\tau}_\parallel^2 \tilde{\Omega}^2 + (1 - 2\tilde{\tau}_\parallel \tilde{\tau}_\perp \tilde{\Omega}^2)\cos(2\tilde{\Omega}\tilde{t}) + (2\tilde{\tau}_\parallel + \tilde{\tau}_\perp)\tilde{\Omega}\sin(2\tilde{\Omega}\tilde{t})]}{8(1 + 4\tilde{\tau}_\parallel^2 \tilde{\Omega}^2)(1 + \tilde{\tau}_\perp^2 \tilde{\Omega}^2)}. \tag{28}$$

Similarly for the third-order problem we have

$$\frac{\partial f_3}{\partial \tilde{t}} = \sin(\tilde{\Omega}\tilde{t}) g_2(\tilde{t}) - \frac{1}{\tilde{\tau}_\perp} f_3(\tilde{t}), \quad \frac{\partial g_3}{\partial \tilde{t}} = -\frac{1}{\tilde{\tau}_\parallel} g_3(\tilde{t}). \tag{29}$$

This is solved to obtain

$$f_3(\tilde{t}) = -C_1 \tilde{\tau}_\perp^2 \tilde{\Omega}\cos(\tilde{t}\tilde{\Omega}) + C_2\, \tilde{\tau}_\perp \sin(\tilde{t}\tilde{\Omega}) - C_3\, \tilde{\tau}_\perp^2 \tilde{\tau}_\parallel \tilde{\Omega}\cos(3\tilde{t}\tilde{\Omega}) + C_4 \tilde{\tau}_\perp^2 \tilde{\tau}_\parallel \sin(3\tilde{t}\tilde{\Omega}), \quad g_3(\tilde{t}) = 0. \tag{30}$$

where

$$C_1 = \frac{2 + \tilde{\tau}_\parallel \tilde{\tau}_\perp + 4\tau_\parallel^3 \tilde{\tau}_\perp \tilde{\Omega}^2 + 2\tilde{\tau}_\perp^2 \tilde{\Omega}^2 + \tilde{\tau}_\parallel^2 \{1 + \tilde{\Omega}^2 [8 + \tilde{\tau}_\perp^2 (8\tilde{\Omega}^2 - 1)]\}}{2(1 + 4\tilde{\tau}_\parallel^2 \tilde{\Omega}^2)(1 + \tilde{\tau}_\perp^2 \tilde{\Omega}^2)^2}, \tag{31}$$

$$C_2 = \frac{4 + 8\tau_\parallel^3 \tilde{\tau}_\perp \tilde{\Omega}^2 + 4\tilde{\tau}_\perp^2 \tilde{\Omega}^2 + \tilde{\tau}_\parallel \tilde{\tau}_\perp (3 - \tilde{\tau}_\perp^2 \tilde{\Omega}^2) + 4\tilde{\tau}_\parallel^2 \tilde{\Omega}^2 [4 + \tilde{\tau}_\perp^2 (4\tilde{\Omega}^2 - 1)]}{4(1 + 4\tilde{\tau}_\parallel^2 \tilde{\Omega}^2)(1 + \tilde{\tau}_\perp^2 \tilde{\Omega}^2)^2}, \tag{32}$$

$$C_3 = \frac{-2\tilde{\tau}_\perp + \tilde{\tau}_\parallel (3\tilde{\tau}_\perp^2 \tilde{\Omega}^2 - 1)}{2(1 + 4\tilde{\tau}_\parallel^2 \tilde{\Omega}^2)(1 + \tilde{\tau}_\perp^2 \tilde{\Omega}^2)^2 (1 + 9\tilde{\tau}_\perp^2 \tilde{\Omega}^2)}, \tag{33}$$

$$C_4 = \frac{-1 + \tilde{\tau}_\perp \tilde{\Omega}^2 (8\tilde{\tau}_\parallel + 3\tilde{\tau}_\perp)}{4(1 + 4\tilde{\tau}_\parallel^2 \tilde{\Omega}^2)(1 + \tilde{\tau}_\perp^2 \tilde{\Omega}^2)^2 (1 + 9\tilde{\tau}_\perp^2 \tilde{\Omega}^2)}. \tag{34}$$

From the solutions to the zeroth- to third-order problems we may infer that $f_n = 0$ if n is odd and $g_n = 0$ if n is even. Then, according to (22), we have

$$\begin{aligned} f(\tilde{t}) = {} & \tilde{\tau}_\perp \frac{\cos(\tilde{\Omega}\tilde{t}) + \tilde{\Omega}\tilde{\tau}_\perp \sin(\tilde{\Omega}\tilde{t})}{2(1 + \tilde{\tau}_\perp^2 \tilde{\Omega}^2)} \varepsilon \\ & + [-C_1 \tilde{\tau}_\perp^2 \tilde{\Omega}\cos(\tilde{t}\tilde{\Omega}) + C_2\, \tilde{\tau}_\perp \sin(\tilde{t}\tilde{\Omega}) \\ & - C_3\, \tilde{\tau}_\perp^2 \tilde{\tau}_\parallel \tilde{\Omega}\cos(3\tilde{t}\tilde{\Omega}) + C_4 \tilde{\tau}_\perp^2 \tilde{\tau}_\parallel \sin(3\tilde{t}\tilde{\Omega})]\varepsilon^3 + O(\varepsilon^5). \end{aligned} \tag{35}$$

We are interested in evaluating the intrinsic magnetoviscosity, defined as in Ref. [15] and which is given by

$$\tilde{\eta}_m = \frac{\eta_m}{\eta_0} = \frac{3}{4} \mathrm{Mn}^{-1} f(\tilde{t}). \tag{36}$$

Substituting (35) in (36), the intrinsic magnetoviscosity can be expressed as

$$\begin{aligned} \tilde{\eta}_m = {} & \frac{3}{4} \varepsilon \mathrm{Mn}^{-1} \left\{ \frac{\cos(\tilde{\Omega}\tilde{t}) + \tilde{\Omega}\tilde{\tau}_\perp \sin(\tilde{\Omega}\tilde{t})}{2(1 + \tilde{\tau}_\perp^2 \tilde{\Omega}^2)} \tilde{\tau}_\perp \right. \\ & + [-C_1 \tilde{\tau}_\perp^2 \tilde{\Omega}\cos(\tilde{t}\tilde{\Omega}) + C_2\, \tilde{\tau}_\perp \sin(\tilde{t}\tilde{\Omega}) \\ & - C_3\, \tilde{\tau}_\perp^2 \tilde{\tau}_\parallel \tilde{\Omega}\cos(3\tilde{t}\tilde{\Omega}) + C_4 \tilde{\tau}_\perp^2 \tilde{\tau}_\parallel \sin(3\tilde{t}\tilde{\Omega})]\varepsilon^2 \\ & \left. + O(\varepsilon^4) \right\}. \end{aligned} \tag{37}$$

Next we recognize that, in the infinitely dilute limit,

$$\mathrm{Mn}^{-1}\varepsilon = \frac{\mathrm{Mn}^{-1}\mathrm{Pe}}{2} = 2\alpha L(\alpha). \tag{38}$$

Substituting Eqs. (16), (18), and (38) into (37) and keeping only the first term in the regular perturbation solution, we obtain

$$\tilde{\eta}_m = \frac{3}{2} \frac{\alpha L^2(\alpha)}{\alpha - L(\alpha)} \frac{\sin(\tilde{\Omega}\tilde{t}) - \tilde{\Omega}\tilde{\tau}_\perp \cos(\tilde{\Omega}\tilde{t})}{(1 + \tilde{\Omega}^2 \tilde{\tau}_\perp^2)} + O(\varepsilon^2). \tag{39}$$

Applying Eq. (10), we obtain the following forms for the nondimensional in-phase $\tilde{\eta}'$ and out-of-phase $\tilde{\eta}''$ dynamic magnetoviscosity:

$$\begin{aligned} \tilde{\eta}'_m &= \left[\frac{3}{2} \frac{\alpha L^2(\alpha)}{\alpha - L(\alpha)} \right] \frac{1}{1 + \tilde{\Omega}^2 \tilde{\tau}_\perp^2}, \\ \tilde{\eta}''_m &= \left[\frac{3}{2} \frac{\alpha L^2(\alpha)}{\alpha - L(\alpha)} \right] \frac{\tilde{\Omega}^2 \tilde{\tau}_\perp^2}{1 + \tilde{\Omega}^2 \tilde{\tau}_\perp^2}. \end{aligned} \tag{40}$$

In obtaining Eq. (40) from Eq. (37) we have chosen to keep, for simplicity, only the leading order term $[O(\varepsilon)]$. In this case the response is seen to be purely sinusoidal. However, we note that inspection of Eq. (37) demonstrates that deviations from purely sinusoidal behavior are predicted as Pe increases. These deviations are seen as additional harmonic contributions [terms with $\cos(3\tilde{\Omega}\tilde{t})$ and $\sin(3\tilde{\Omega}\tilde{t})$ in Eq. (37)] which would correspond to higher-order ($n > 1$) in-phase $\tilde{\eta}'_{m,n}$ and out-of-phase $\tilde{\eta}''_{m,n}$ magnetoviscosities.

These expressions in Eq. (40) for the in-phase and out-of-phase components of the magnetoviscosity are similar to the model for the dynamic viscosity of a Maxwell fluid, but with a field-dependent relaxation time given by (17) and a field-dependent viscosity equal to $\eta_m = \frac{3}{2} \frac{\alpha L^2(\alpha)}{\alpha - L(\alpha)} \eta\phi$. The Maxwell model describes the viscoelastic behavior of a material using simple mechanical elements such as a spring and a dashpot. This model is acceptable as a first approximation to relaxation

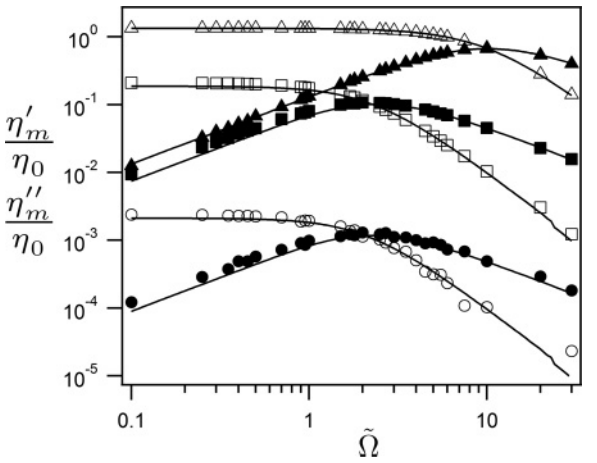

FIG. 1. In-phase and out-of-phase magnetoviscosity for different Langevin parameters and Pe = 1. Markers correspond to simulation results. For the in-phase dynamic magnetoviscosity, open circles (○) correspond to $\alpha = 0.1$, open squares (□) to $\alpha = 1.0$, and open triangles (△) to $\alpha = 10.0$. For the out-of-phase dynamic magnetoviscosity, closed circles (●) correspond to $\alpha = 0.1$, closed squares (■) to $\alpha = 1.0$, and closed triangles (▲) to $\alpha = 10.0$. The straight line (—) corresponds to Eq. (40).

behavior. If we use the same model to interpret our results, it is clear that the magnetic torque corresponds to the spring while the rotational fluid drag corresponds to the dashpot, and the characteristic time is equal to the field-dependent transverse relaxation time of the nanoparticles.

B. Numerical Solution

The numerical solution of Eq. (21) was obtained using the ODE45 function in MATLAB. This function implements a Runge-Kutta method with a variable time step for efficient computation. The algorithm solves the equations and yields the time-dependent magnetoviscosity. The dynamic in-phase and out-of-phase magnetoviscosities were obtained through numeric implementation of Eq. (11) using the trapezoidal rule.

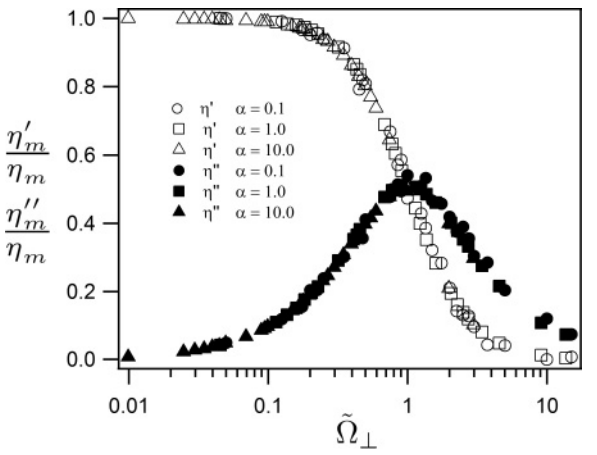

FIG. 2. Normalized in-phase, η'_m/η_m, and out-of-phase, η''_m/η_m, dynamic magnetoviscosity for Pe = 1, obtained from simulations, reduced to a master curve using the dimensionless effective frequency, $\tilde{\Omega}_\perp$.

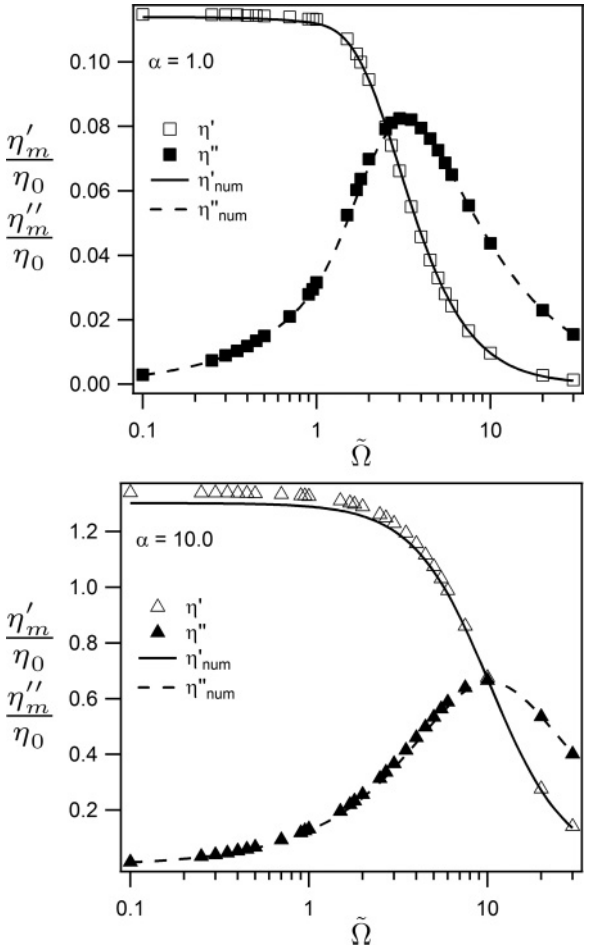

FIG. 3. In-phase and out-of-phase magnetoviscosity at Pe = 5 for different Langevin parameters for simulation (markers) and numerical results (solid and dotted lines).

This was found to give satisfactory values owing to the small time step size used for numerical output ($\Delta\tilde{t} = 0.001$).

IV. COMPARISON OF SIMULATIONS AND CONTINUUM MODELING

The dynamic magnetoviscosity as a function of shear oscillation frequency for different Langevin parameters and for Pe = 1.0 is shown in Fig. 1. First, it is noticeable that the dynamic magnetoviscosity increases with increasing magnetic field. Also, as the magnetic field increases, there is a displacement of the crossover frequency for the in-phase and out-of-phase dynamic viscosities to higher frequencies, indicating a decrease of the ferrofluid relaxation time with increasing magnetic field. At frequencies below the crossover η' dominates, indicating viscous behavior, but at higher frequencies η'' dominates, indicating an elastic character to the magnetoviscosity. A comparison with the analytical solution of MRS is also shown for $\varepsilon = 0.5$. The solution agrees with the simulation results for all Langevin parameters, but deviations are seen at higher frequencies for $\alpha = 0.1$. For Pe < 1 we do not see a significant effect of Pe on the simulated dynamic viscosity, consistent with Eq. (40).

Another approach for the interpretation of the shear and magnetic field dependence of the dynamic viscosity of

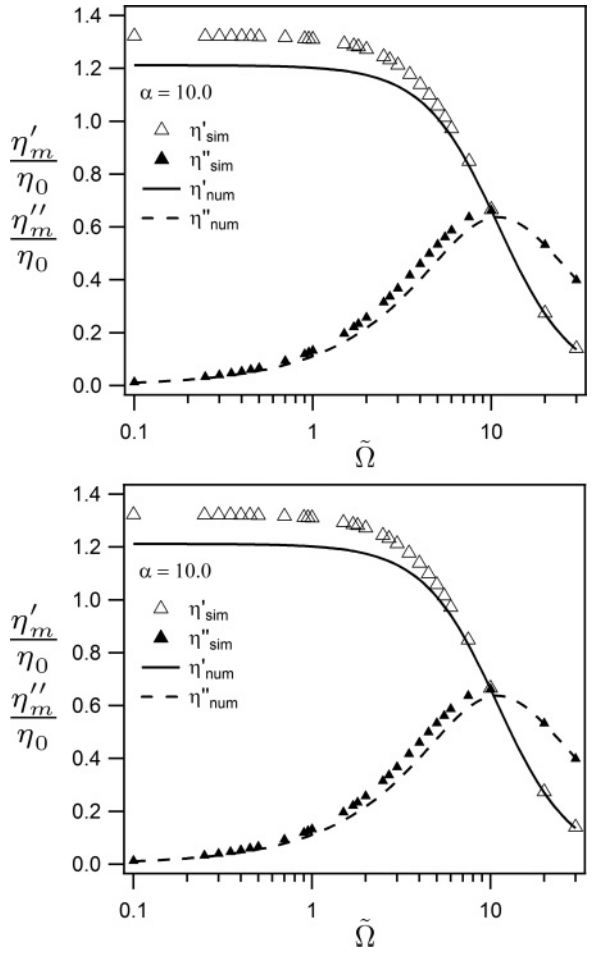

FIG. 4. In-phase and out-of-phase magnetoviscosity for Pe = 10 at different Langevin parameters for simulation (markers) and numerical results (solid and dotted line).

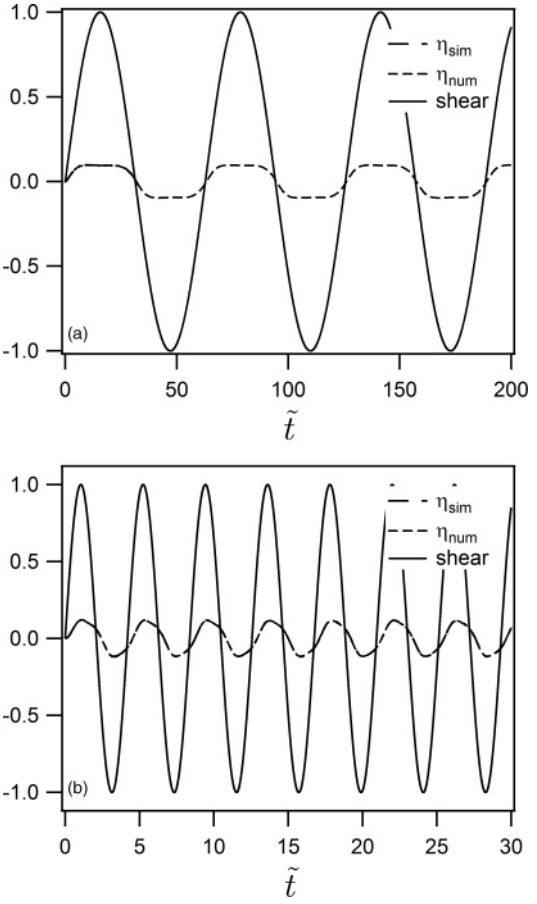

FIG. 5. Magnetoviscosity as a function of time for Pe = 5 and $\alpha = 1.0$ and for (a) $\tilde{\Omega} = 0.1$ and (b) $\tilde{\Omega} = 1.5$. The results of simulations and numerical solution are indistinguishable.

ferrofluids is the use of characteristic dimensionless parameters that capture the basic physics of the phenomena. As shown in Fig. 2, using the transverse relaxation time Eq. (17), it is possible to define a new scaled frequency $\tilde{\Omega}_\perp = 2\Omega\tau_\perp$ with which all the simulation results for Pe < 1 collapse into a single curve.

The oscillatory rheological behavior of the ferrofluid at high shear is shown in Fig. 3 for Pe = 5 and Fig. 4 for Pe = 10. For both Péclet values it is found that the crossover point shifts to higher frequencies as the magnetic field increases, indicating a decrease of the characteristic time of the ferrofluid response to the oscillatory shear. However, if we interpret the frequency of the peak in $\tilde{\eta}'_m$ as an inverse relaxation time, we find that the field dependence of this relaxation time is no longer given by Eq. (17) for $\tau_\perp$. For Pe = 10.0 (Fig. 4), before the $\tilde{\eta}'_m$ and $\tilde{\eta}''_m$ crossover, there is a clear peak in the $\tilde{\eta}'_m$ curve and $\tilde{\eta}''_m$ becomes higher in magnitude than $\tilde{\eta}'_m$, indicative of a viscous-elastic transition with respect to frequency. A comparison with the numerical solution for Eq. (21) is also shown. It is appreciable that the magnetoviscosity obtained by numerical solution of the governing equations using the MRS equation quantitatively agrees with simulations for both Péclet numbers and different Langevin parameters. It also predicts the viscous-elastic transition shown for Pe = 10. However, as the Langevin parameter increases, there is a quantitative deviation of the numerical solution compared with the simulation results in the $\tilde{\eta}'_m$ curve, indicating that the MRS magnetization relaxation equation is no longer able to quantitatively predict dilute ferrofluid behavior in an oscillating shear flow.

Breakdown of agreement between simulations and predictions using the MRS equation is further evident when comparing the time dependence of the magnetoviscosity predicted using the two approaches, as shown in Figs. 5 to 8. Figure 5 illustrates oscillatory but not sinusoidal response to the sinusoidal shear flow for Pe = 5.0 and $\alpha = 1.0$. It also shows that sinusoidal response in the magnetoviscosity is recovered at higher applied fields ($\alpha = 10.0$). In Figs. 5 and 6 the agreement between simulations and numerical solution using the MRS equation is such that the two curves superimpose. This is also true in Fig. 7 for Pe = 10.0 and $\alpha = 1$, where again it is seen that the magnetoviscosity response is not sinusoidal under these conditions. Sinusoidal response is again recovered for higher applied fields, as shown in Fig. 8 for Pe = 10 and $\alpha = 10$; however, this figure also shows deviation between the predictions of simulations and the numerical solution. Interestingly, Figs. 5 and 7 correspond to Mn > 1 whereas Figs. 6 and 8 correspond to Mn < 1. As noted before, the Mason number represents the ratio of viscous to magnetic stresses, hence these observations indicate that, when the viscous stresses dominate the magnetic stresses, deviations

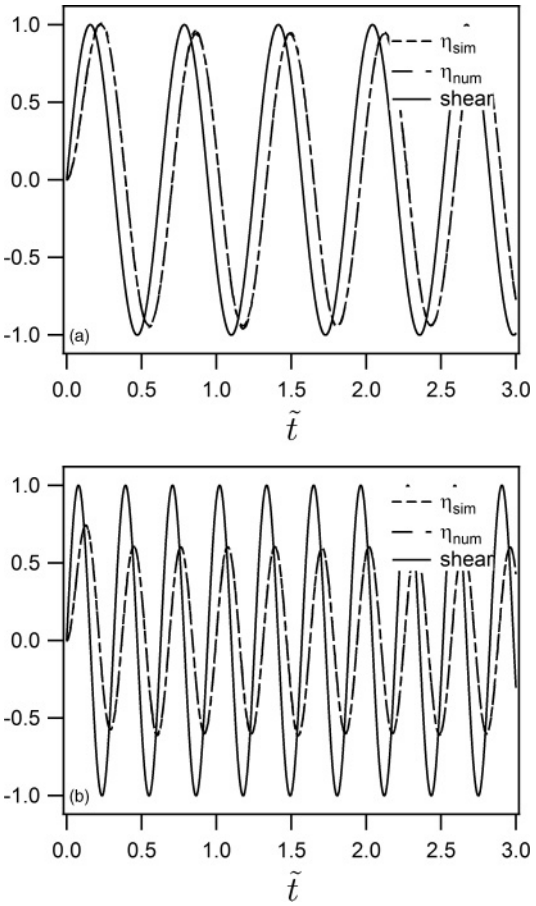

FIG. 6. Magnetoviscosity as a function of time for Pe = 5 and $\alpha = 10.0$ and for (a) $\tilde{\Omega} = 10.0$ and (b) $\tilde{\Omega} = 20.0$. The results of simulations and numerical solution are indistinguishable.

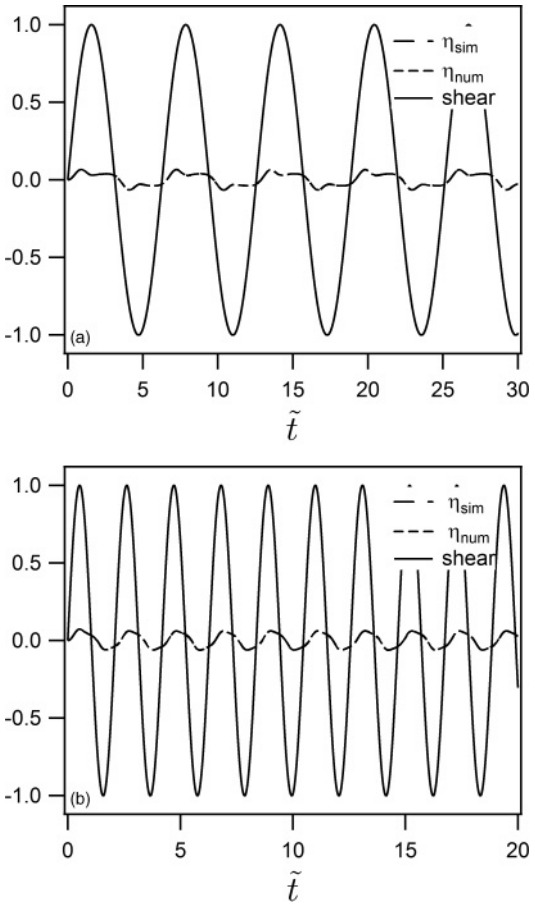

FIG. 7. Magnetoviscosity as a function of time for Pe = 10 and $\alpha = 1.0$ and for (a) $\tilde{\Omega} = 1.0$ and (b) $\tilde{\Omega} = 3.0$. The results of simulations and numerical solution are indistinguishable.

may occur from purely sinusoidal magnetoviscous response of a dilute ferrofluid to a sinusoidal oscillating shear flow.

V. CONSIDERATION OF THE COX-MERZ RULE FOR DILUTE FERROFLUIDS

The Cox-Merz rule [57] states that $\eta(\dot{\gamma}) = \eta^*(\Omega)$ when $\Omega = \dot{\gamma}$, where $\eta(\dot{\gamma})$ is the viscosity at a steady shear rate, and $\eta^*(\Omega)$ is the dynamic viscosity at oscillating frequency Ω obtained from small amplitude oscillatory shear experiments. The dynamic viscosity is obtained from the in-phase and out-of-phase viscosities using

$$\eta_m^* = [(\eta_m')^2 + (\eta_m'')^2]^{\frac{1}{2}}. \tag{41}$$

Note that, by using the MRS equation, the steady-state magnetoviscosity in a constant magnetic field and shear flow is precisely given by [9]

$$\eta_m = \frac{3}{2}\frac{\alpha L^2(\alpha)}{\alpha - L(\alpha)}\eta_0\phi. \tag{42}$$

In our case, using Eq. (40) in Eq. (41) it can be easily shown that

$$\eta_m^* = \eta_m\left[\left(\frac{1}{1+\Omega^2\tau_\perp^2}\right)^2 + \left(\frac{\Omega\tau_\perp}{1+\Omega^2\tau_\perp^2}\right)^2\right]^{\frac{1}{2}} = \eta_m, \tag{43}$$

demonstrating that the Cox-Merz rule applies for dilute ferrofluids under conditions for which Pe $\ll 2$. However, under these conditions the magnetoviscosity is independent of shear rate, making the result rather trivial. Next we consider the applicability of the Cox-Merz rule for higher shear rates by comparing the simulation results of the present contribution to those of our previous work [13] for the steady shear magnetoviscosity. To do so we consider the case where the oscillatory shear flow is given by

$$\dot{\gamma} = \gamma_0\Omega\sin(\Omega t). \tag{44}$$

Note that this is the same as Eq. (1) with $\dot{\gamma}_0 = \gamma_0\,\Omega$, hence the rotational Péclet number is now Pe $= \gamma_0\tilde{\Omega}$ and the frequency is nondimensionalized with respect to the rotational diffusion coefficient D_r. For simplicity, in our simulations we used $\gamma_0 = 1$. The frequency varied from 0.1 to 100.0 and the Langevin parameters used were $\alpha =$ [0.1, 1.0, 3.0, 5.0, 10.0, 15.0, 20.0, 30.0]. Figure 9 shows the complex viscosity calculated from Eq. (41) as a function of frequency and the steady-state viscosity (from [13]) as a function of shear rate. It is shown that, in the limit of low shear rate and low frequency, the dynamic viscosity and the steady-state viscosity are similar, indicating that the Cox-Merz rule applies under these conditions. However, as the frequency increases the complex viscosity decreases faster than the

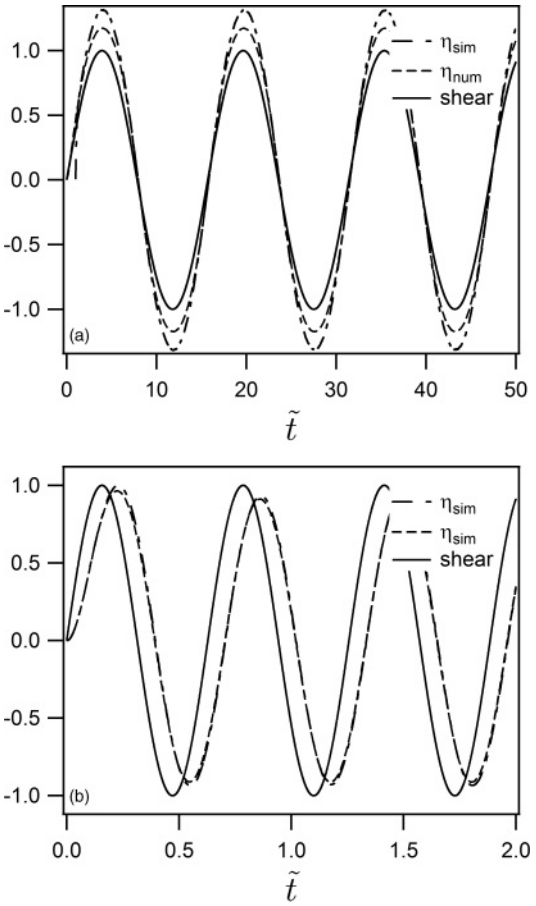

FIG. 8. Magnetoviscosity as function of time for Pe $= 10$ and $\alpha = 10.0$ and for (a) $\tilde{\Omega} = 0.4$ and (b) $\tilde{\Omega} = 20.0$.

steady-state magnetoviscosity as a function of Pe. Thus, at higher shear rates the Cox-Merz rule ceases to apply.

VI. CONCLUSIONS

The dynamic properties of dilute ferrofluids under oscillatory shear and constant magnetic fields were studied using Brownian dynamic simulations and continuum modeling using the ferrohydrodynamics equations. Results show that the in-phase and out-of-phase components of the complex magnetoviscosity depend on both magnetic field strength and the frequency and magnitude of the sinusoidal oscillatory shear wave. Even though we are considering the infinitely dilute limit in which there are negligible particle-particle interactions (and therefore no particle chaining), the results indicate an apparent elastic character to the rheology of these suspensions. At small rotational Péclet number a regular perturbation solution of the continuum equations shows that the response of the magnetoviscosity follows a Maxwell-like model with field-dependent viscosity and characteristic time equal to the field-dependent transverse relaxation time. A numerical solution of the ferrohydrodynamics equations was also obtained. Comparison between the numerical solution and simulations shows that the magnetoviscosity obtained using the kinetic magnetization relaxation equation agrees with simulations for a wide range of Péclet number and Langevin parameter, but deviates from the simulations at high values of the Langevin parameter. The Cox-Merz rule for dilute ferrofluids was evaluated using an asymptotic analytical solution of the ferrohydrodynamics equations, valid for Pe $\ll 2$. It was demonstrated that the Cox-Merz rule applies for dilute ferrofluids under conditions of small shear rates but does not apply at higher shear rates.

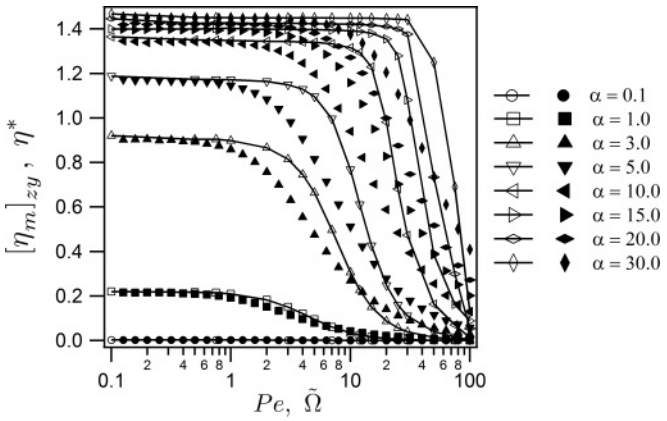

FIG. 9. Steady shear magnetoviscosity and complex magnetoviscosity as a function of shear rate (Pe) and frequency($\tilde{\Omega}$), respectively. Open markers are for the steady-state magnetoviscosity while closed markers are for the complex magnetoviscosity.

ACKNOWLEDGMENTS

This work was supported by the US National Science Foundation CAREER program (CBET- 0547150) and the NSF Nanoscale Science and Engineering Center on Templated Synthesis and Assembly at the Nanoscale (DMR-0832760).

[1] R. E. Rosensweig *et al.*, J. Colloid Interface Sci. **29**, 680 (1969).
[2] J. P. McTague, J. Chem. Phys. **51**, 133 (1969).
[3] A. Zeuner *et al.*, Phys. Rev. E **58**, 6287 (1998).
[4] A. O. Ivanov *et al.*, Phys. Rev. E **75**, 061405 (2007).
[5] H. Shahnazian and S. Odenbach, J. Phys. Condens. Matter **20**, 204137 (2008).
[6] D. Y. Borin and S. Odenbach, J. Phys. Condens. Matter **21**, 246002 (2009).
[7] M. I. Shliomis, Sov. Phys. JETP **34**, 1291 (1972).
[8] Y. L. Raikher and M. I. Shliomis, Sov. Phys. JETP **4**, 41 (1974).
[9] M. A. Martsenyuk *et al.*, Sov. Phys. JETP **38**, 413 (1974).
[10] A. Zubarev and L. Y. Iskakova, Colloid J. **65**, 703 (2003).
[11] J. A. Kupriyanova and A. V. Zatovsky, J. Mol. Liq. **127**, 102 (2006).
[12] A. Yu Zubarev and L. Yu Iskakova, Physica A **382**, 378 (2007).
[13] D. Soto-Aquino and C. Rinaldi, Phys. Rev. E **82**, 046310 (2010).
[14] J. H. Sanchez and C. Rinaldi, Phys. Fluids **22**, 043304 (2010).
[15] J. H. Sanchez and C. Rinaldi, J. Colloid Interface Sci. **331**, 500 (2009).
[16] G. Bossis *et al.*, Prog. Colloid Polym. Sci. **81**, 251 (1990).

[17] B. U. Felderhof, Phys. Rev. E **62**, 3848 (2000).
[18] B. U. Felderhof, Magnetohydrodynamics **37**, 307 (2001).
[19] M. I. Shliomis, Phys. Rev. E **64**, 063501 (2001).
[20] X. He *et al*., J. Appl. Phys. **97**, 10Q302 (2005).
[21] P. Ilg, M. Kroger, and Siegfried Hess, J. Magn. Magn. Mater. **289**, 325 (2005).
[22] M. I. Shliomis and K. I. Morozov, Phys. Fluids **6**, 2855 (1994).
[23] H. Brenner, J. Colloid Interface Sci. **32**, 141 (1970).
[24] H. Brenner and M. H. Weissman, J. Colloid Interface Sci. **41**, 499 (1972).
[25] S. R. Strand and S. Kim, Rheol. Acta **31**, 94 (1992).
[26] J. C. Bacri *et al*., Phys. Rev. Lett. **75**, 2128 (1995).
[27] A. Chaves *et al*., Phys. Rev. Lett. **96**, 194501 (2006).
[28] V. M. Zaitsev and M. I. Shliomis, J. Appl. Mech. Tech. Phys. **10**, 696 (1969).
[29] R. E. Rosensweig *et al*., J. Magn. Magn. Mater. **85**, 171 (1990).
[30] O. G. Calderón and S. Melle, J. Phys. D **35**, 2492 (2002).
[31] S. Rhodes *et al*., J. Electrost. **64**, 513 (2006).
[32] J. P. Embs *et al*., Phys. Rev. E **73**, 036302 (2006).
[33] D. Soto-Aquino and C. Rinaldi, J. Magn. Magn. Mater. **323**, 1319 (2011).
[34] D. Borin *et al*., J. Magn. Magn. Mater. **323**, 1273 (2011).
[35] L. RG, *Structure and Rheology of Complex Fluids* (Oxford University Press, New York, 1998).
[36] S. Chatrchyan *et al*., Journal of Instrumentation **5** (2010).
[37] J. Claracq *et al*., Rheol. Acta **43**, 38 (2004).
[38] D. J. Klingenberg, J. Rheol. **37**, 199 (1992).
[39] M. Parthasarathy and D. J. Klingenberg, Mater. Sci. Eng., R **17**, 57 (1996).
[40] D. J. Klingenberg *et al*., J. Rheol. **51**, 883 (2007).
[41] H. Kanai and T. Amari, Rheol. Acta **32**, 539 (1993).
[42] W. H. Li *et al*., Mater. Sci. Eng. A **371**, 9 (2004).
[43] B. J. de Gans *et al*., Phys. Rev. E **60**, 4518 (1999).
[44] B.-J. de Gans *et al*., Faraday Discuss. **112**, 209 (1999).
[45] S. T. Milner, J. Rheol. **40**, 303 (1996).
[46] B. S. Chae *et al*., Rheol. Acta **40**, 599 (2001).
[47] S. Odenbach, *Magnetoviscous Effects in Ferrofluids* (Springer, Berlin, 2002).
[48] M. Pinho, B. Brouard, J. M. Génevaux, N. Dauchez, O. Volkova, H. Mézière, and P. Collas, J. Magn. Magn. Mater. **323**, 2386 (2011).
[49] H. Goldstein *et al*., *Classical Mechanics*, 3rd ed. (Addison Wesley, San Francisco, 2002).
[50] H. C. Ottinger, *Stochastic Processes in Polymeric Fluids* (Springer, Berlin, 1996).
[51] R. E. Rosensweig, *Ferrohydrodynamics* (Cambridge University Press, New York, 1985).
[52] R. Moskowitz and R. E. Rosensweig, Appl. Phys. Lett. **11**, 301 (1967).
[53] A. Chaves *et al*., Phys. Fluids **20**, 053102 (2008).
[54] S. Khushrushahi and M. Zahn, J. Magn. Magn. Mater. **323**, 1302 (2011).
[55] M. Miwa *et al*., Tribol. Lett. **15**, 97 (2003).
[56] M. T. L. López *et al*., Croatica Chemica Acta **80**, 445 (2007).
[57] W. P. Cox and E. H. Merz, J. Polym. Sci. **28**, 619 (1958).